NASA TECHNICAL NOTE

NASA TN D-4986

NASA TN D-4986

AN OPTICAL SYSTEM FOR RECORDING SCHLIEREN IMAGES WITH A CONTINUOUS-WRITING ULTRA-HIGH-SPEED FRAMING CAMERA

by Lemuel E. Mauldin III and E. Conrad Compton

Langley Research Center
Langley Station, Hampton, Va.

NATIONAL AERONAUTICS AND SPACE ADMINISTRATION • WASHINGTON, D. C. • JANUARY 1969

NASA TN D-4986

AN OPTICAL SYSTEM FOR RECORDING SCHLIEREN IMAGES WITH A CONTINUOUS-WRITING ULTRA-HIGH-SPEED FRAMING CAMERA

By Lemuel E. Mauldin III and E. Conrad Compton

Langley Research Center
Langley Station, Hampton, Va.

NATIONAL AERONAUTICS AND SPACE ADMINISTRATION

For sale by the Clearinghouse for Federal Scientific and Technical Information
Springfield, Virginia 22151 – CFSTI price $3.00

AN OPTICAL SYSTEM FOR RECORDING SCHLIEREN IMAGES WITH A CONTINUOUS-WRITING ULTRA-HIGH-SPEED FRAMING CAMERA

By Lemuel E. Mauldin III and E. Conrad Compton
Langley Research Center

SUMMARY

An optical system for recording schlieren images with a continuous-writing framing camera has been developed and used successfully. The integrated system comprising the ultra-high-speed camera, the f/8 Z-light-path schlieren system, the focusing lenses, the square-wave-pulse light generator, and the two-beam knife-edge assembly affords up to 72 consecutive schlieren photographs at a recording rate up to 1 200 000 frames per second. The generator provides selectable pulse durations of 60, 250, and 1000 microseconds. This controlled-duration light source eliminates the need for an elaborate high-speed shutter normally used with continuous light sources. A two-beam knife-edge assembly splits the Z-type schlieren beam into two separate and complete schlieren images of the test area and directs them into the camera. The system has provided good quality pictures of supersonic particles and hypersonic gas flow.

INTRODUCTION

In hypervelocity particle and flow research facilities there are many instances where a significant number of sequenced, ultra-high-speed (above 50 000 frames per second) schlieren photographs are needed. Various ultra-high-speed cameras, such as the Miller rotating-mirror camera, the Cranz-Schardin camera, and the lenticular plate Nipkow disk camera, have the potential of satisfying the framing speed requirement but cannot be used directly with the conventional Z-light-path schlieren method. The lenticular plate camera (ref. 1) offers advantages of a large number of frames and a large aperture, and the Cranz-Schardin camera offers advantages of very brief framing times and a large aperture. Both cameras would require modified schlieren systems and would have the disadvantage of scrambling the pictures which, in turn, would require an unscrambling process to obtain the correct sequence. The rotating-mirror camera when operating in the range from 10^5 to 10^7 frames per second can produce more satisfactory pictures than most other ultra-high-speed cameras if enough light is available. These cameras can be used over a wider range of magnification (up to ×100), for silhouette or self-luminous objects, and the continuous access eliminates synchronization problems even in unpredictable events (ref. 2).

One of the rotating-mirror cameras can provide up to 80 sequenced photographs at recording rates up to 1 440 000 frames per second. However, the optical layout and small effective aperture of this camera have prevented it from being used to make schlieren photographs in the usual manner. Ordinarily, the image of the test section is focused onto the film plane of the camera. This camera, however, has a beam-splitting prismatic mirror behind the objective lens which splits the image of a schlieren beam (unless at the knife-edge location) since schlieren light is directional. A solution would be to use the prismatic mirror as the knife-edge to prevent image splitting but this solution proved to be impractical since the camera had to be moved to position the knife-edge and there was no way of viewing the knife-edge cutoff with the camera loaded for a test. An alternative would be to project the image on a ground-glass screen and photograph the screen, but the high f-number (f/26) of the camera and limited intensity from a point light source (required for schlieren system) preclude this method. The problem was solved by splitting the beam external to the camera with a prismatic mirror which could be easily positioned. There was still a requirement for a light source intense enough to expose the film at the shortest exposure times and also to be capable of being turned on and off so that there would be no multiple exposure problems (being a continuous-writing device the framing camera can rewrite). For this particular application a point-source light system capable of reliable operation in a continuous or controlled pulse mode was desired. The light source desired has a diameter of 0.8 millimeter or less, output durations of 60, 250, and 1000 microseconds (for recording rates of 1 200 000, 300 000, and 75 000 frames per second), and sufficient brightness to expose properly ASA 125 film when a f/8 Z-light-path schlieren system is used. This report describes the development of the square-wave-pulse light generator and specialized schlieren system.

SYMBOLS

Optical

M	mirror
i	image
l	lens
p	object distance, meters (see fig. 6)
q	image distance, meters (see fig. 6)

Numerical subscript with a symbol indicates the item.

Electrical

C	capacitance, farads
E	charging voltage, volts
I	current, amperes
J	energy, joules
L	inductance, henrys
N	number of pulse-forming network (PFN) sections
R	resistance, ohms
T	duration of light source, seconds
t	time, seconds
Z	impedance, ohms
α	damping ratio
ω	frequency, radians per second

Subscripts:

L	load
T	total
i	characteristic or internal
m	impedance matching
n	nth peak in current waveform

o initial value (at $t = 0$)

r rise

APPARATUS

A schematic of the integrated system is shown in figure 1. The system is composed of an ultra-high-speed framing camera, an f/8 Z-light-path schlieren system, a two-beam knife-edge assembly, focusing lenses, and a square-wave-pulse light generator (light source).

Ultra-High-Speed Framing Camera

A simplified optical schematic of the Miller type framing camera is shown in figure 2. The camera can record transient events up to 1 440 000 frames per second with a maximum turbine speed of 6000 revolutions per second. The camera has an effective aperture of f/26 at the film plane and can record 80 frames spaced at equal time increments. The optical system includes a 61-centimeter-focal-length objective lens in a focusing mount, a fixed prismatic mirror, a rotating prismatic mirror, and over 400 other optical elements to achieve framing. (Figure 2 shows some of the optical elements for two frames.) The incoming light is routed to two sides of a turbine driven prismatic mirror which alternately sweeps the top bank of frames with the top beam and the bottom bank of frames with the bottom beam. The sweep may start at any frame on either bank and continue until all frames are exposed.

Knife-Edge Assembly and Focusing-Lens Mount

The two-beam knife-edge assembly is shown in figure 3. The ray trace indicates the function of each optical element. The beam from M_2 is focused on the vertex of a small porro prism (the 90° knife-edge vertex, of schlieren quality, is formed by two silvered surfaces 3.2 millimeters wide by 12.7 millimeters long). This porro prism is then the knife-edge of the schlieren system. The prism is positioned so that the reflection angles of the incoming beams from M_2 are equal. The light is reflected by the prism faces to two small flat mirrors mounted with their surfaces parallel to the respective faces of the prism and positioned so that the center lines of the beams are approximately 16 millimeters apart. Reflected from the flat mirrors, the beams are collimated by using two 19.1-millimeter-diameter, 101.6-millimeter-focal-length lenses. These two lenses can be moved in two mutually perpendicular axes.

Located between the camera objective lens and the knife-edge assembly are two 40-millimeter-diameter, 572-millimeter-focal-length focusing lenses. These lenses are

mounted as a unit (fig. 4) and can be positioned in the vertical direction. These two lenses are cut so that they can be placed close together while maintaining the optical axis of each lens needed for individual beam control. After passing through the focusing lenses, the beams are directed into the camera objective lens.

Square-Wave-Pulse Light Generator

A square-wave-pulse light generator was designed for nominal durations of 60 microseconds, 250 microseconds, and 1 millisecond. These pulses allow shuttering of the continuous-writing camera at 1 200 000 frames per second, 300 000 frames per second, and 75 000 frames per second, respectively. This method of shuttering the camera has proved to be more practical than mechanically shuttering continuous light when photographing nonluminous or slightly luminous events (refs. 3 to 5). The square-wave light pulses are formed by discharging artificial transmission lines (also referred to as pulse-forming network or PFN) through a short-arc xenon lamp. The PFN is electrically matched to the light source.

A block diagram of the square-wave-pulse light generator is shown in figure 5. A standard xenon short-arc-lamp power supply is used for continuous operation of the lamp to aline and adjust the schlieren system. The pulse mode is used for taking photographs after the schlieren system has been alined. A 0-to-300-volt dc power supply is used to charge the PFN. The PFN is terminated with the short-arc lamp and an impedance matching nichrome resistance wire. The light pulse is synchronized to the event with a silicon controlled rectifier trigger unit that is gated by an oscilloscope signal. The point source is reimaged and sharpened with a 0.8-millimeter-diameter aperture. The light pulse shape is monitored and recorded with a photocell, oscilloscope, and oscilloscope-camera combination.

DESIGN APPROACH

Criteria

The usual method of schlieren photography is to focus the schlieren image onto the film plane of the camera. The framing camera used, however, differs from most other cameras in that a beam-splitting prismatic mirror behind the objective lens divides the light from the lens into two beams before the image is formed. This arrangement provides two complete images from the original light beam. However, a special condition must be satisfied where an image from a schlieren system is concerned. The light beam from a schlieren system already has direction and if the beam is divided at any place except at the precise image of the source (i.e., at the knife-edge location), the resultant images will be only parts of the complete image. A solution would be to use the beam-splitting prismatic mirror as the knife-edge. This method would be impractical, however,

since the entire camera (which weighs 680 kilograms) would have to be moved for proper positioning of the knife-edge. An alternative would be to project the schlieren image on a ground-glass screen and photograph the screen, but the high f-number (f/26) of the camera and limited intensity from a point light source (required for schlieren system) preclude this method. Another alternative would be to divide the beam with a prismatic mirror external to the camera. A mirror external to the camera could be positioned easily for knife-edge adjustments, and the two beams could be routed to each side of the beam-splitting mirror in the camera. Design criteria for such a system are as follows:

(1) Provide some means for splitting the recording beam into two separate and complete recording beams with a prismatic mirror of sufficient sharpness to function as a schlieren-system knife-edge, and direct both beams in the same direction and parallel to each other, and keep both path lengths equal

(2) Determine what optics are needed to direct the light beams through the camera optics without vignetting

(3) Determine to what extent the optics required will degrade image quality

(4) Develop a suitable high-intensity light source (square-wave pulse) to provide enough light over the exposure time required for both film tracts.

Schlieren System

In a Z-light-path schlieren system such as that shown in figure 1, the knife-edge can only be positioned in the vertical direction at the tangential focus of M_2 and in the horizontal direction at the sagittal focus of M_2 for uniform shading of the light. If the knife-edge is positioned at any other point or in another direction, the image is not complete. If a prism is used at either of the correct positions to bisect the point for the knife-edge, then two complete images are obtained. With any change in the density of the medium of the tunnel test section, light passing through this gradient is refracted in such a way as to cause brighter or darker points of the schlieren display image depending on whether the light from these points is refracted away from or towards either of the two prism faces. Therefore, disturbances represented in one schlieren image are opposite in contrast to disturbances represented in the other image. The two beams are reflected by the prism to the two small folding flat mirrors and from these mirrors to the collimating lenses shown in figure 3. The flat mirrors are positioned to insure equal light path lengths and to place the image on the optical axis of each lens. The distance selected between the two collimating lenses establishes the separation of the two beams until intercepted by the camera prism.

Figure 6 shows the light-source ray trace (solid lines) of one beam of the two-beam system. The light-source rays are collimated by l_1. This collimation conserves the

light over the relatively long path to the focusing lens l_2. The collimation is poor due to the short focal length of l_1, but this is not a degrading factor. The focusing lens l_2 and camera objective lens l_3 converge the light to an image of the light source near the face of the fixed prismatic mirror in the camera. This convergence is necessary for the beam to be routed through the camera optics with minimum vignetting.

Also presented in figure 6 is the test-section ray trace (dash lines) with images of the model indicated by heavy arrows and object distances and image distances for each lens represented by p and q, respectively. Exact location of the model image is given by using the following lens formula:

$$\frac{1}{p} + \frac{1}{q} = \frac{1}{f} \tag{1}$$

where f is the focal length in meters.

The "object" of the collimating lens l_1 is the image of the test section i_1 formed by M_2. The image i_2 formed by l_1 is the "object" for the focusing lens l_2. Using standard sign convention, the "object" distance p_1 is negative since the "object" lies on the same side of l_1 as the image formed by l_1. Because the "object" distance p_2 is within the focal length of l_2, the image formed by l_2 will be a virtual image i_3 and will be on the same side of l_2 as is p_2 since q_2 is negative. Therefore, i_3 appears to l_3 to be coming from more than 7 feet away. This reimaging was a primary purpose of the focusing lens since the camera can only focus on objects beyond 7 feet.

The focusing lenses are positioned relative to the camera objective lens so that the test section is in focus at the film plane. The lens diopter rating is chosen for maximum magnification without vignetting as the beam traverses the camera optical path. The distances between the knife-edge assembly, focusing lenses, and camera objective lens will vary depending on work space available.

The alinement of the camera with the schlieren system is very critical and painstaking because of the long light path from the knife-edge to the film plane. The camera has to be accurately positioned to minimize vignetting of the filmed image, that is, positioned so that the entire light beam is used and not spilled over at the various optical elements. Once the camera is positioned the images to be recorded are brought into focus in the film plane by moving the focusing-lens assembly to the proper location in the light path. Although 1.75-diopter lenses were used as the focusing lenses, 1.5-diopter lenses could have been used to provide greater magnification. With this larger image, however, the alinement problem would become increasingly more critical.

Another disadvantage to the overall system is the knife-edge arrangement where the sensitivity is fixed for both paths of light. The sensitivity of any schlieren system is inversely proportional to the height of the unobscured portion of the source image. The knife-edge in this system cannot be run in and out of the image for greater sensitivity

without shading one path more than the other. The same intensity for both paths is desirable for the continuous-writing camera. Thus, the sensitivity of this schlieren system is solely dependent on the size of the light source. When the 0.8-millimeter-diameter aperture did not provide sufficient sensitivity, a 0.4-millimeter-diameter aperture was used. This 0.4-millimeter-diameter aperture is not recommended where sensitivity is not a problem since the smaller aperture reduces the light intensity and requires more critical system alinement.

Evaluation of Xenon Short-Arc Lamp

A 75-watt, three-terminal, high-pressure xenon lamp for reliable pulsing at energies up to 10 joules is the light source in this system. Luminous efficiency is 20 lumens/watt and typical luminous flux is 1500 lumens as rated by the manufacturer. Since the arc length is 0.4 millimeter, the lamp can be used as a point source for schlieren application.

To determine whether the lamp could properly expose film with the two-beam schlieren system, exposure tests were made. The turbine in the camera was positioned so that one frame in the camera was illuminated. Exposures were made at graduated electrical energy levels with a conventional flash-lamp circuit (fig. 7), first with a schlieren system having a ground-glass screen and then with the two-beam schlieren system. To avoid the possibility of error that might be introduced by reciprocity law failure, the duration of the flash was tailored to correspond to the exposure duration at the various specified framing rates. After the energy required to expose one frame of the film was determined in this way, it was then multiplied by 180 to estimate the electrical energy needed to expose all 80 frames of the record and to account for the interframe dead time. This procedure was repeated for several types of film and film developer. At electrical energies which produced the correct exposure, a radiometer measured integrated luminous energy. These readings were also multiplied by 180 to estimate the luminous energy needed to expose properly an 80-frame record. For example, when an ASA 125 film and a high activity developer were used, an electrical energy of 0.025 joule was needed to expose properly one frame with 4.5 joules estimated to be needed to expose all 80 frames with the two-beam schlieren system. At this electrical energy, a radiometer measured 0.366 lumen-second/meter^2 for one frame with 66 lumen-seconds/meter^2 estimated to be the luminous energy for all 80 frames. Data for other types of film are discussed in the section entitled "Results and Discussion."

Pulse-Forming Network

A pulse-forming network (PFN) is a lumped parameter equivalent to a lossless transmission line (refs. 6 and 7) and consists of capacitor-inductor sections as shown in figure 8. In this figure the PFN is terminated with a matched load formed by a short-arc lamp and an impedance matching resistor.

Since the PFN charges and discharges as a transmission line, then the network can best be understood by using transmission-line characteristics. A transmission line charged to a voltage level E and then connected to a load equal to its characteristic impedance Z_i will discharge as a rectangular voltage pulse of amplitude $E/2$ and a rectangular current pulse (ref. 8) of amplitude $E/2Z_i$. The load voltage drops to one-half the initial voltage since the network appears to the load as a voltage source E in series with the line's characteristic impedance Z_i. The sudden drop in voltage at the load is equivalent to a negative voltage step $-E/2$ which propagates toward the open end and decreases the line voltage to $+E/2$ as it travels. The step wave is reflected at the open end without phase reversal and proceeds back toward the load end until the line is discharged. The net result is a rectangular pulse whose amplitude is one-half the initial charging voltage E and whose duration is twice the one-way propagation time through the network (ref. 9). This mechanism is shown pictorially in figure 9.

If the load is not matched to the transmission line, however, the wave will be partially reflected at the load instead of being completely dissipated. Depending on the mismatch ratio, the wave will be reflected as a positive or negative step. This reflection traverses the line toward the open end, is totally reflected there without changing sign, and travels back toward the load. The reflections will continue in this manner until all the stored energy in the line is dissipated. The series of steps will have the same sign if $Z_L > Z_i$ but will be alternate in sign if $Z_L < Z_i$.

Pulse width measurements are made from the 70 percent points so that ideal transmission-line equations may be applied (refs. 10 and 11). The equations used in the design of a pulse forming network are as follows:

$$Z_i = \sqrt{\frac{L_T}{C_T}} \tag{2}$$

$$T = 2\sqrt{L_T C_T} \tag{3}$$

$$C_T = \frac{T}{2Z_i} \tag{4}$$

$$L_T = \frac{TZ_i}{2} \tag{5}$$

$$t_r = \frac{T}{2N} \tag{6a}$$

or expressed in percent equation (6a) is

$$\frac{t_r}{T} = \frac{100}{2N} \tag{6b}$$

$$J = \frac{C_T E^2}{2} \tag{7}$$

Other factors also affect PFN design. Equation (2) shows that capacitance varies inversely with the square of the characteristic impedance of the line. To design a line to match a short-arc lamp having a conductive resistance anticipated to be less than 0.1 ohm would require an impractical amount of capacitance. Since energy varies directly with the capacitance and square of the voltage (eq. (7)), the capacitance must be minimized to flash the lamp at optimum anode voltage and remain within the 10-joule maximum energy limit of the lamp. This means that a PFN must be designed for a characteristic impedance larger than the lamp and matched to the lamp with an external resistance. On the other hand, the line inductance varies directly with the square of the line characteristic impedance and a large inductance cannot be tolerated. Internal resistance in long lengths of coil wire required for large inductances causes the pulse to droop. This problem has been solved in the 1-millisecond line by using high permeability coil forms to reduce the number of coil turns. The number of line sections cannot be chosen indiscriminately but must be chosen for the total line capacitance and capacitors available. Equation (6b) shows, however, that at least five sections should be used for a rise time of less than 10 percent of pulse length. The final design, therefore, must be a compromise involving these factors.

The pulse forming networks were designed around 8-microfarad, 14-microfarad, and 32-microfarad capacitors since they could easily be obtained. Design parameters for the PFN's are shown in table I. The resistance of the short-arc lamp was calculated to be less than 0.1 ohm by the method presented in the appendix. Therefore, the resistance of the impedance matching nichrome wire resistors was chosen to be 0.1 ohm less than the characteristic impedance of the PFN's. All coils were wound with 14-gage magnet wire. Because of the high currents involved, 14-gage wire was also used for the nichrome resistance wire and all lead wires from the PFN to the short-arc lamp. Since a switch capable of carrying the required current would be impractical, switching from one PFN to another was accomplished by changing two lead wires.

RESULTS AND DISCUSSION

The estimates of electrical energy and integrated luminous energy for proper film exposure shown in table II indicate that the photographic system can properly expose several types of film with two types of film developer. For example, an electrical energy of only 1.8 joules is needed with this system to expose properly ASA 400 film with a high activity developer. For comparison, if the same camera were used with a ground-glass-screen schlieren system, more than 50 times this electrical energy would be needed which would exceed the maximum energy capability of the lamp. The two-beam system is well within the maximum energy limits. In the future, it may be possible to use a ground-glass-screen schlieren system with the camera if a short-arc lamp is developed with

higher maximum energy limits or better luminous efficiency. Of the two types of 35-millimeter film tested, ASA 125 film was chosen because of the finer grain. Although this film requires almost three times as much energy for correct exposure as the ASA 400 film with the same developers, this energy is well within the safe energy limit of the lamp. Of the two film developers tested, the high activity developer was used since a lower electrical energy could be used to obtain similar resolution.

Since the short-arc lamp is new to PFN applications, no data describing the conductive resistance of the lamp were given by the manufacturer. The method for calculating conductive resistance of an ordinary flashtube does not apply to the short-arc lamp since the short-arc lamp conductive resistance does not control total discharge loop resistance. In addition, the small loop resistance causes an underdamped, oscillatory discharge waveform as opposed to a highly damped, nonoscillatory discharge waveform for the flashtube circuit. Therefore, transient analysis was used to measure the conductive resistance. The method is not accurate, but this is not a serious obstacle in matching the PFN properly. The lamp resistance found from the capacitor discharge is not necessarily the same as that in a PFN discharge where the peak current is held to a steady value for a much longer time. However, this resistance measurement did provide a first approximation to the characteristics of the short-arc lamp when used with PFN's.

As shown in figure 10, the conductive resistance of the short-arc lamp is very small and decreases rapidly with increasing pulse energy. This small nonlinear resistance would be difficult if not impossible to match properly to a PFN. Therefore, a nichrome resistance wire which was placed in series with the lamp complemented the small resistance of the lamp to match a much larger PFN characteristic impedance. This nichrome wire resistor, which makes up almost all the load, outweighs the nonlinear effect of the lamp. Thus, the load is essentially matched over a range of operating energy. On the other hand, almost all the PFN energy is dissipated in the wire. This loss of energy is not detrimental, however, since the small amount of energy used by the lamp is within the safe energy limits and produces enough light for proper film exposure.

The square-wave light pulses produced by the three PFN's which properly expose ASA 125 film with high activity developer (see section entitled "Evaluation of Xenon Short-Arc Lamp") are shown in figure 11. The 60-microsecond light pulse has a rise time of about 7 percent of the pulse length and allows a camera recording rate of about 1 200 000 frames per second for a 72-frame exposure (i.e., allowing eight frames for rise and fall of the light pulse). The 250-microsecond light pulse has a rise time of about 1 percent of the pulse length and allows a camera recording rate of about 300 000 frames per second. The 1-millisecond light pulse has a rise time of about 4 percent of the pulse length and allows a camera recording rate of about 75 000 frames per second.

The ringing on top of the light pulses is caused by lumped parameter values of capacitance and inductance for the PFN which cannot smoothly simulate the distributed parameters of an actual transmission line. As the number of sections is increased, the ringing frequency increases and the rise time is improved; this produces a more accurate simulation of the ideal transmission line (ref. 12). Originally, the capacitance and inductance for each section was the same. A laboratory test showed, however, that the amplitude of the ringing peaks on top of the waveform could be attenuated by additional inductance at the lamp end of the circuit and that the trailing edge of the pulse could be "squared" considerably by adding additional capacitance to the open end of the circuit. It was also found that the capacitance in the other sections could be varied to produce a more rectangular pulse but only at the expense of increasing the ringing amplitude on top of the pulse. Although the light fluctuations on top of the pulses shown in figure 12 affect the density of the film from frame to frame, this is not a serious degrading factor since the density changes are barely detectable by the human eye. The gradual voltage drop of the pulse is caused by distributed line losses. These line losses are resistive in nature and are mostly contained in the inductance coils. The tail of the pulse is due to a voltage reflection caused by PFN and load impedance mismatch. Since the short-arc lamp has an inherently variable impedance, all impedance mismatch cannot be eliminated. These factors can be minimized by carefully winding the coils for maximum quality factor Q and by matching as closely as possible the short-arc lamp and the series load resistor to the PFN (ref. 4).

The integrated luminous energy estimate of 66 lumen-seconds/meter^2 for proper exposure of ASA 125 film developed in a high activity developer was a conservative estimate compared with the value actually needed. Integration of each area under the light pulse curve shows that approximately 29 lumen-seconds/meter^2 is needed. In actual practice, however, small adjustments had to be made to conform to the peculiarities of each lamp. A PFN charging voltage (usually between 100 and 300 volts) was chosen which provided the most reliable triggering of the lamp and a stable light output. Correct exposure was then obtained by choosing the right neutral density filter and placing it in the light path or by choosing a film-developer combination compatible with the amount of light.

An actual schlieren recording of a 22-caliber bullet traveling at a velocity of about 550 meters/second is shown in figure 12. These pictures were made with the 250-microsecond square-wave-pulse light generator. The first two and last six frames are underexposed and correspond to the rise time and fall time of the pulse, respectively. The middle 50 frames are evenly exposed; these correspond to the flat portion of the pulse. The first 37 frames are recorded with the bottom beam in the camera and the final 21 frames are recorded with the top beam. The shock waves made by the bullet in the first 36 frames are opposite in contrast to the shock waves in the final 21 frames since the knife-edge action is reversed. Six consecutive schlieren photographs of shock flow

around a 10^{o} wedge model in an expansion tube are shown in figure 13. The velocity of the shock flow was 5 kilometers/second and the expansion tube density was 0.0176 kilogram/meter^3. The camera recording rate was 170 000 frames per second. These records demonstrate the compatibility of the light generator, camera, and two-beam schlieren system.

CONCLUDING REMARKS

A unique two-beam schlieren system and a point-source square-wave-pulse light generator with durations of 60 microseconds, 250 microseconds, and 1 millisecond were developed for a continuous-writing framing camera and were used for schlieren recording of ultra-high-speed events. Up to 72 schlieren photographs can be obtained at recording speeds up to 1 200 000 frames per second. The optical design allows the ultra-high-speed camera to be used with a f/8 Z-light-path collimated-beam schlieren system. The square-wave light pulse eliminates the need for an elaborate high-speed shutter mechanism for photographing events that are not self-luminous. The light may be burned continuously for last minute schlieren adjustments and yet be ready for photographing with the pulse modes by switching a mode selector. Two lead changes can select another light pulse and allow a different framing rate. The light output can be varied over a range of intensities to meet proper exposure requirements for several types of film.

Langley Research Center,
National Aeronautics and Space Administration,
Langley Station, Hampton, Va., August 21, 1968,
126-13-03-16-23.

APPENDIX

MEASUREMENT OF SHORT-ARC-LAMP CONDUCTIVE RESISTANCE

The circuit shown in figure 7 was also used to determine the conductive resistance of the short-arc lamp. The anode to cathode voltage is divided by the lamp current to determine the resistance of a flashtube (refs. 13 and 14). For the short-arc lamp, however, this procedure cannot be used. The capacitor discharge circuit – not the short-arc lamp – controlled total loop resistance due to the closely space electrodes. Therefore, a method was used to measure more accurately the resistance of the short-arc lamp.

An oscilloscope and current loop were used to monitor the discharge current as shown in figure 7. A sample oscilloscope display is shown in figure 14(a). The variation in current is that of an exponentially damped sinusoid having a maximum value of $E/\omega L_i$, a constant period of $2\pi/\omega$, and a damping factor of $e^{-\alpha t}$ as shown in figure 14(b). The damping ratio α is defined as

$$\alpha = \frac{R_T}{2L_i} \tag{8}$$

where R_T is the total loop resistance and L_i is the total loop internal inductance. The positive envelope of the curve is given by

$$I = I_o e^{-\alpha t} \tag{9}$$

where I_o is the maximum current envelope value and can be expressed as

$$I_o = \frac{E}{\omega L_i} \tag{10}$$

If I_n represents a positive maximum current occurring at time t_n and I_{n+1} represents a succeeding positive maximum current occurring at time t_{n+1}, then equation (11) can be derived from equation (9) by obtaining values of I_n and I_{n+1} at t_n and t_{n+1} and then taking the ratio; thus,

$$\frac{I_n}{I_{n+1}} = e^{\alpha\left(t_{n+1}-t_n\right)} \tag{11}$$

APPENDIX

Solving for α yields

$$\alpha = \frac{1}{t_{n+1} - t_n} \ln \frac{I_n}{I_{n+1}} \tag{12}$$

where $t_{n+1} - t_n$ is a period of oscillation. Substituting equation (8) into equation (12) and solving for R_T gives

$$R_T = \frac{2L_i}{t_{n+1} - t_n} \ln \frac{I_n}{I_{n+1}} \tag{13}$$

By substituting $\omega = \frac{2\pi}{t_{n+1} - t_n}$ into equation (10), the loop inductance L_i can be expressed as

$$L_i = \frac{E}{\omega I_o} = \frac{E\left(t_{n+1} - t_n\right)}{2\pi I_o} \tag{14}$$

Substituting equation (14) into equation (13) yields

$$R_T = \frac{E}{\pi I_o} \ln \frac{I_n}{I_{n+1}} \tag{15}$$

Now, E is known and I_n and I_{n+1} can be found from an oscilloscope current trace as shown in figure 14(a). The maximum envelope current value I_o can be found by solving for α in equation (12) and substituting the resulting value with other measured values into equation (9). Thus,

$$I_o = I_n e^{\alpha t_n} \tag{16}$$

The conducting lamp resistance can be found by solving for R_T when the lamp is not in the circuit (capacitor short circuited) and subtracting this value from R_T found when the lamp is in the discharge path.

REFERENCES

1. Coleman, K. R.: Ultra-High-Speed Photography. Reports on Progress in Physics, Vol. XXVI, Inst. Phys. Phys. Soc. (London), 1963, pp. 269-305.

2. Courtney-Pratt, J. S.: A Review of the Methods of High-Speed Photography. Reports on Progress in Physics, Vol. XX, Phys. Soc. (London), 1957, pp. 379-432.

3. Griffin, William C.: A High-Intensity Electronic Light Source for High-Speed Cameras. J. SMPTE, vol. 66, no. 3, Mar. 1957, pp. 127-129.

4. Crapo, B. J.; Hill, L. L.; and Marshall, T.: A High-Intensity Rectangular-Pulse Light Source for High-Speed Photography. U.S. Nav. Ord. Lab. paper presented at Fifth International Congress on High-Speed Photography (Washington, D.C.), Oct. 16-22, 1960.

5. Courtney-Pratt, J. S.; and Thackeray, D. P. C.: Apparatus for High Speed Photography. Univ. of Cambridge, Sept. 1956.

6. Jess, J.; and Schüssler, H. W.: On the Design of Pulse-Forming Networks. IEEE Trans. Circuit Theory, vol. CT-12, no. 3, Sept. 1965, pp. 393-400.

7. Carlin, H. J.: Cascaded Transmission Line Synthesis. RADC-TR-61-157, U.S. Air Force, Apr. 27, 1961.

8. White, H. J.: Gillette, P. R.; and Lebacqz, J. V.: The Pulse-Forming Network. Pulse Generators, First ed., G. N. Glasoe and J. V. Lebacqz, eds., McGraw-Hill Book Co., Inc., 1948, pp. 175-224.

9. Smith, H.; and Oray, T.: Nomogram Simplifies Pulse-Forming Network Design. EEE – Circuit Design Eng., vol. 11, no. 8, Aug. 1963, pp. 56-57.

10. Warner, D. F.: The Application of Large Capacitors for Use in Energy Storage Banks. Capacitor Facts No. 4, Gen. Elec. Co.

11. Schmidt, D. F.; and Wilson, S. R., eds.: The Application of Pulse-Forming Networks. Capacitor Facts No. 8, Gen. Elec. Co.

12. Yevtyanov, S. I.; and Red'kin, G. Ye.: Investigation of Pulse Shape in an Artificial-Line Modulator. Telecommun. Radio Eng., no. 3, (pt. 2, vol. 21), Mar. 1966, pp. 106-111.

13. Edgerton, Harold E.: Xenon Flash Lamp Design. Advances in Quantum Electronics. Jay R. Singer, ed., Columbia Univ. Press, 1961, pp. 276-287.

14. Heard, H. G.: Variation of Arc Resistance and Arc Power With Current in Pulsed Xenon Optical Pump Lamps. Proc. IEEE (Correspondence), vol. 51, no. 9, Sept. 1963, pp. 1234-1235.

TABLE I.- PARAMETERS USED IN CONSTRUCTION OF 60-, 250-, AND 1000-MICROSECOND PULSE FORMING NETWORKS

Parameter	Light-source duration of –		
	60 μsec	250 μsec	1000 μsec
C_T, microfarads . . .	56	252	512
L_T, microhenrys . . .	15.4	63.0	512.0
No. of PFN sections . .	7	18	8
Z_i, ohms	0.5	0.5	1.0
R_m, ohms	0.4	0.4	0.9

TABLE II.- LAMP AND LUMINOUS ENERGY FOR PROPER EXPOSURE OF THREE FILM-DEVELOPER COMBINATIONS WITH THE TWO-BEAM SCHLIEREN SYSTEM

Film	Film developer	Electrical energy, J	Integrated luminous energy, $\frac{\text{lm-sec}}{\text{m}^2}$
ASA 400	High activity	1.8	15.1
ASA 125	High activity	4.7	29.1
ASA 125	Fine grain	9.0	43.1

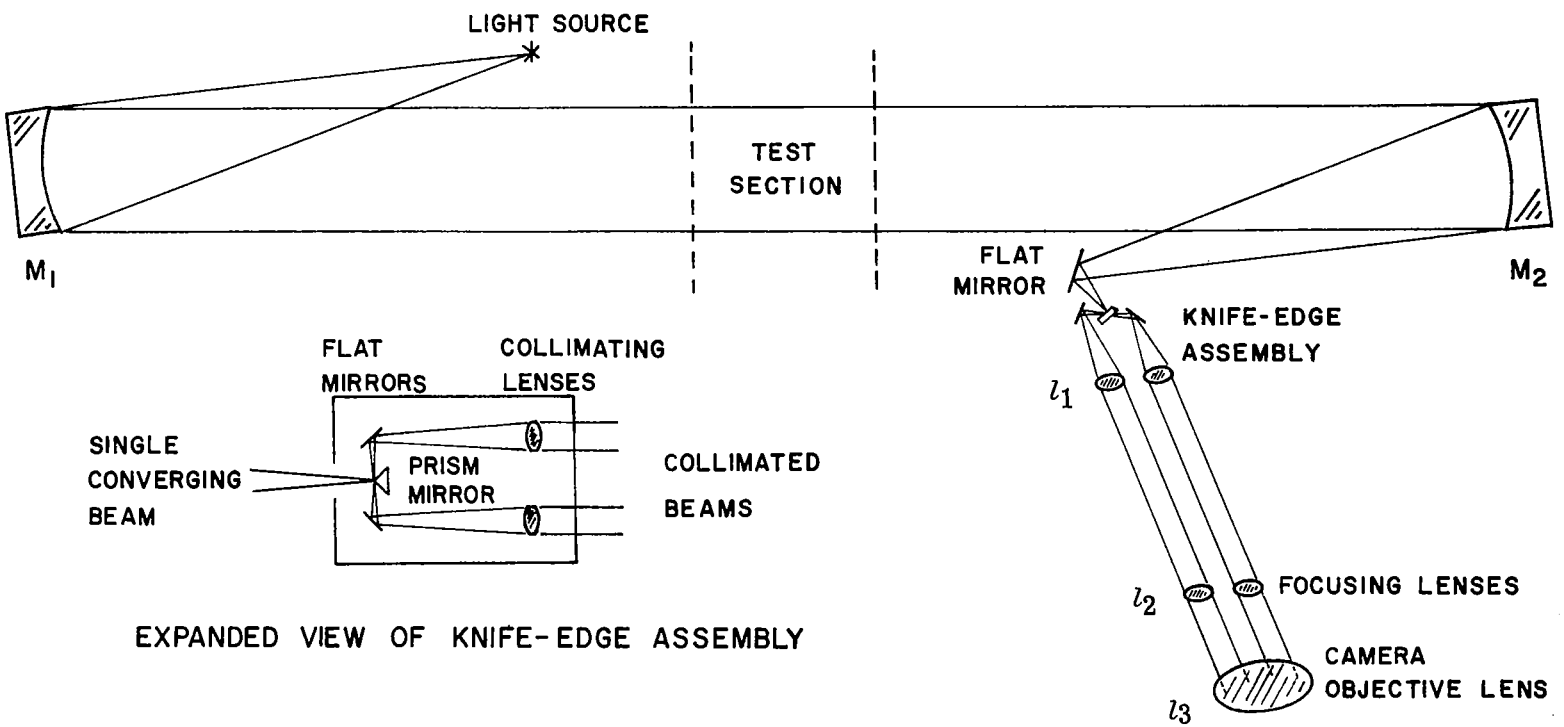

Figure 1.- Two-beam schlieren system.

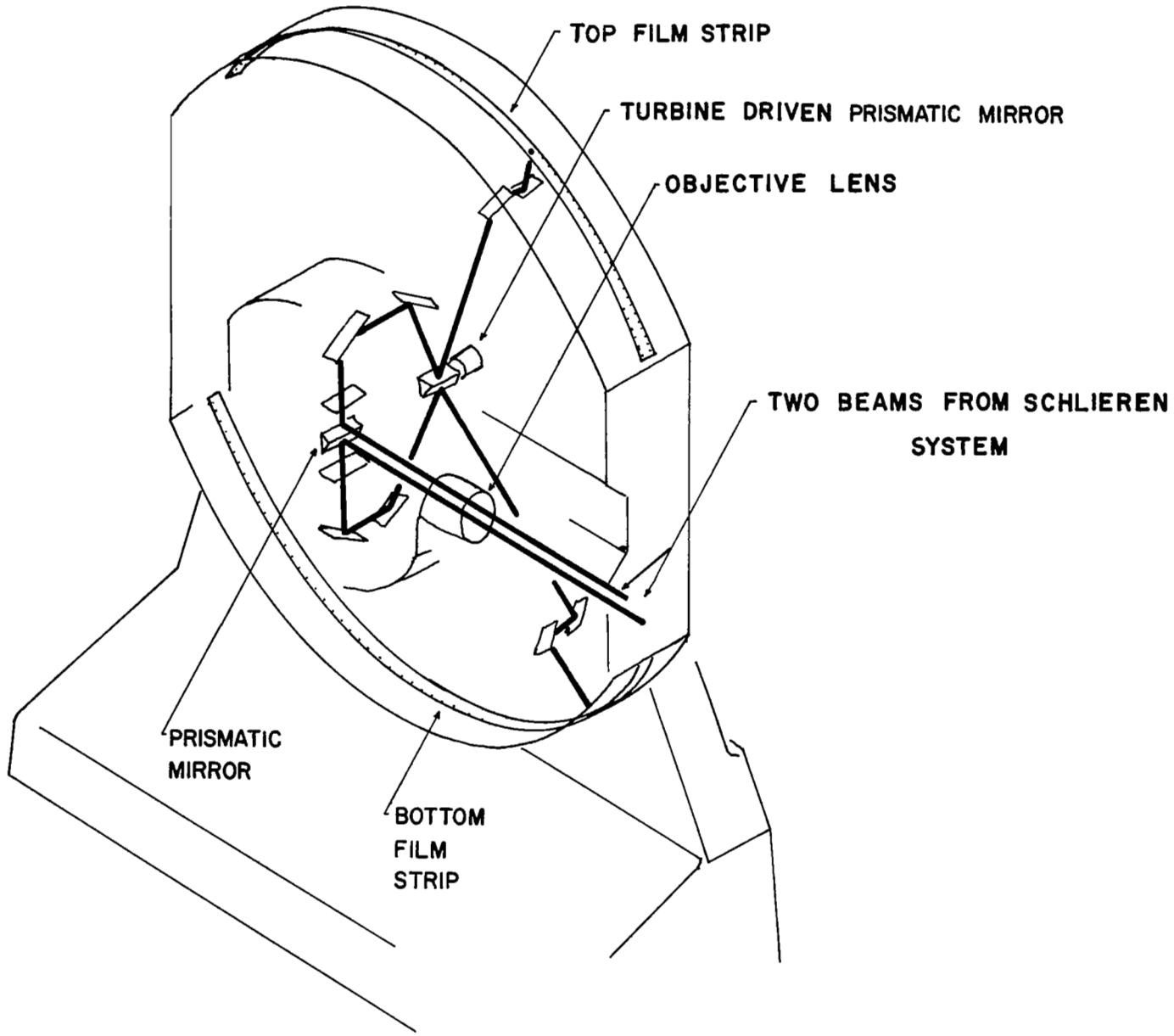

Figure 2.- Simplified optical schematic of ultra-high-speed framing camera.

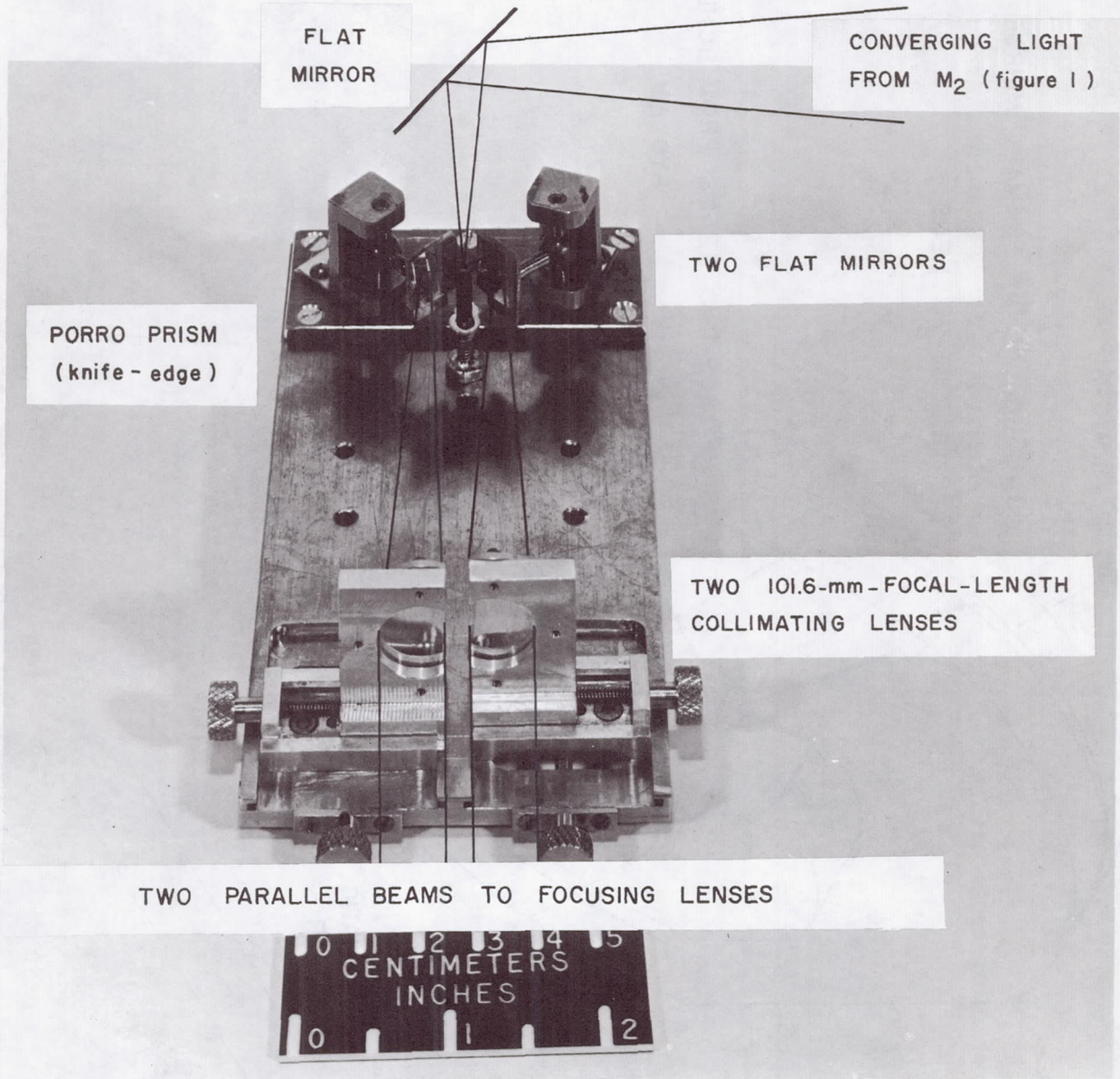

Figure 3.- Ray trace of two-beam knife-edge assembly. L-66-10197.1

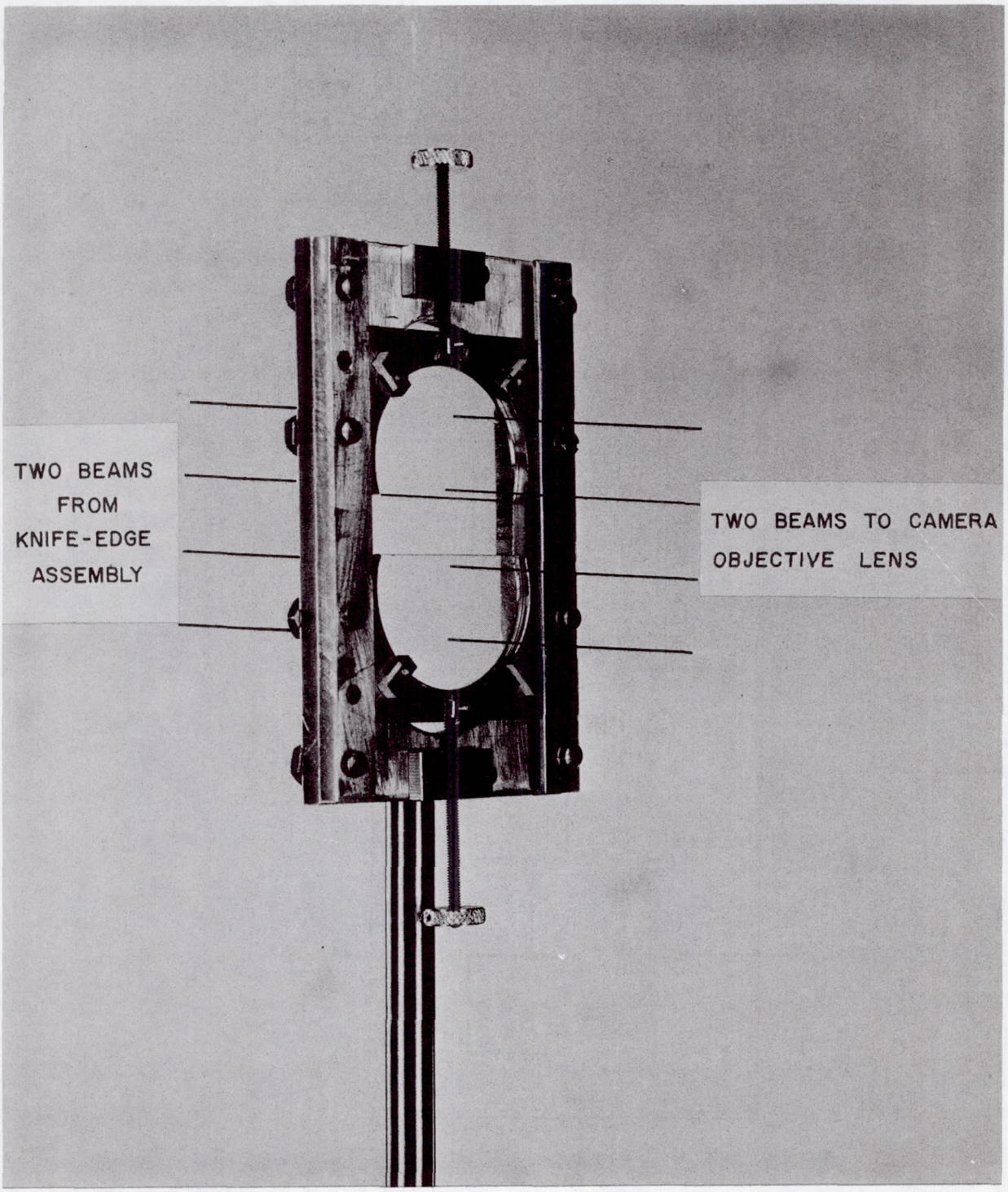

Figure 4.- Vertical mounting of focusing lenses. L-67-5786.1

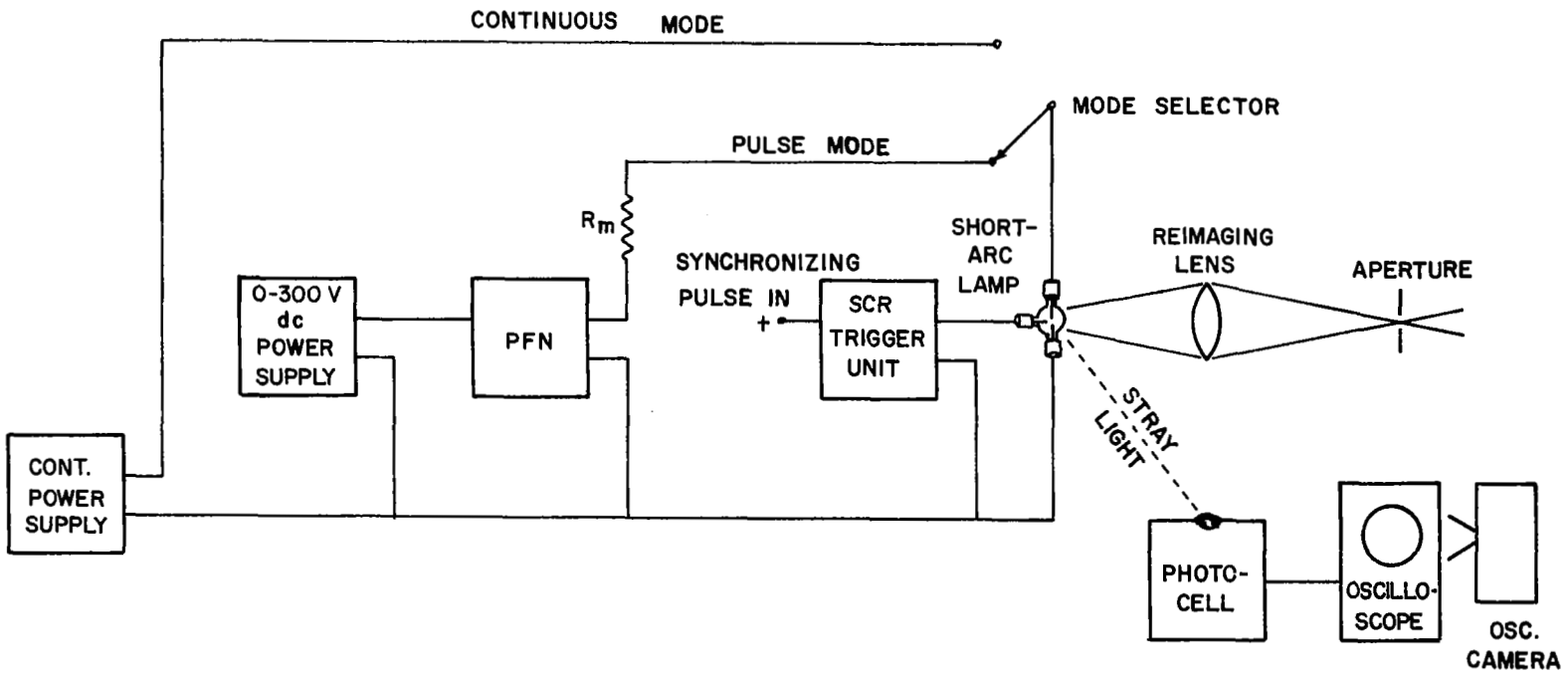

Figure 5.- Block diagram of square-wave-pulse light generator.

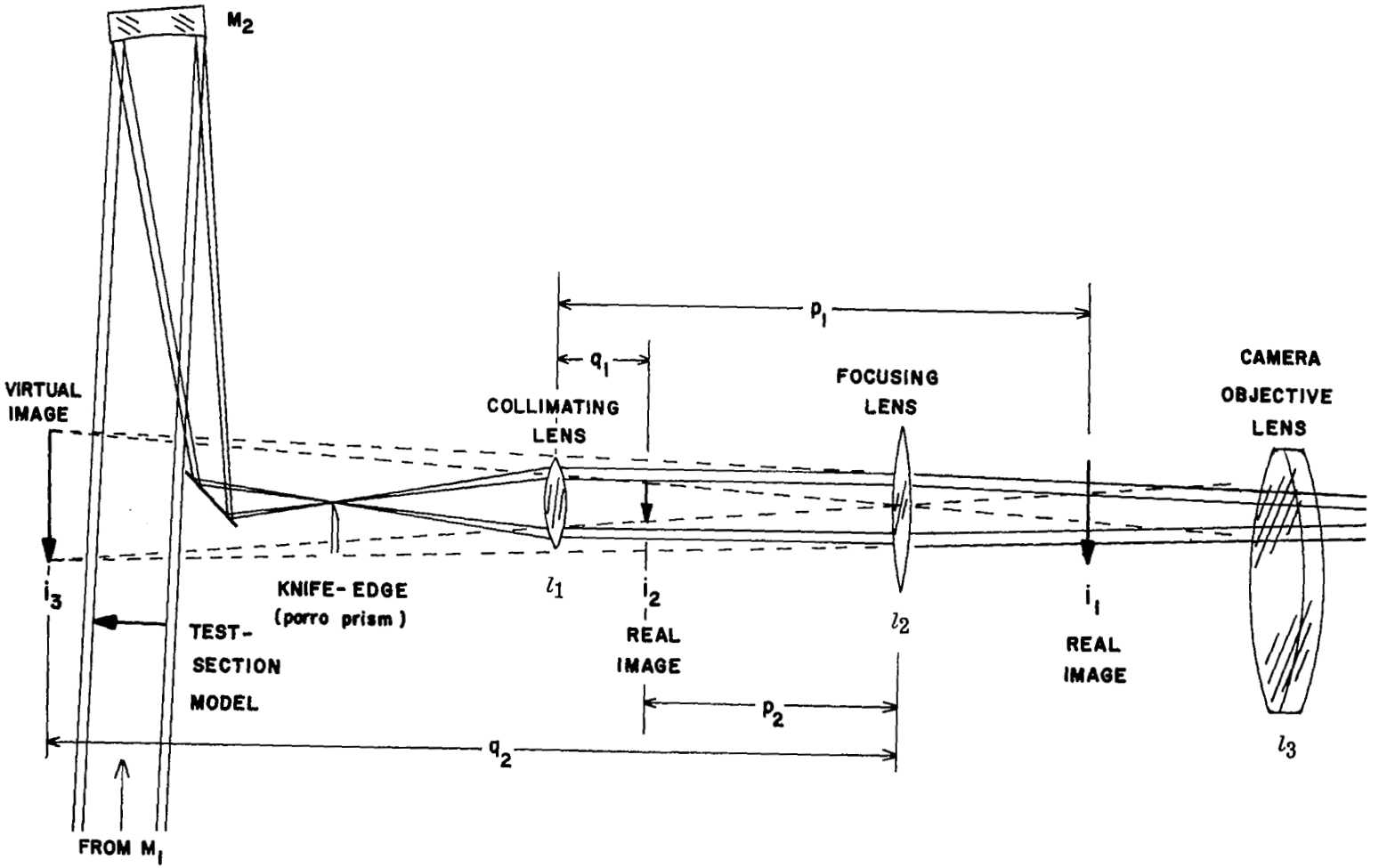

Figure 6.- Ray trace of one schlieren beam showing location of the model images formed by l_1 and l_2.

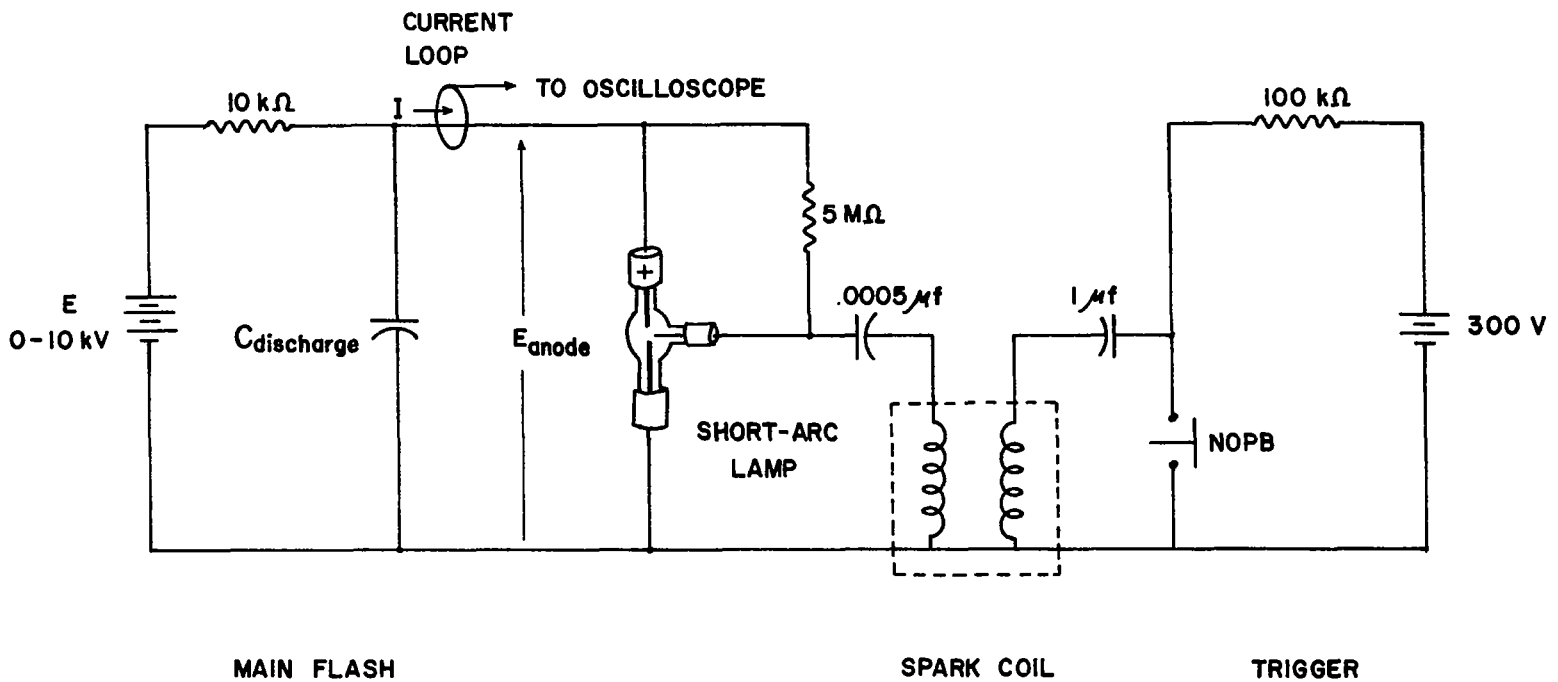

Figure 7.- Typical flash-lamp circuit used in exposure tests.

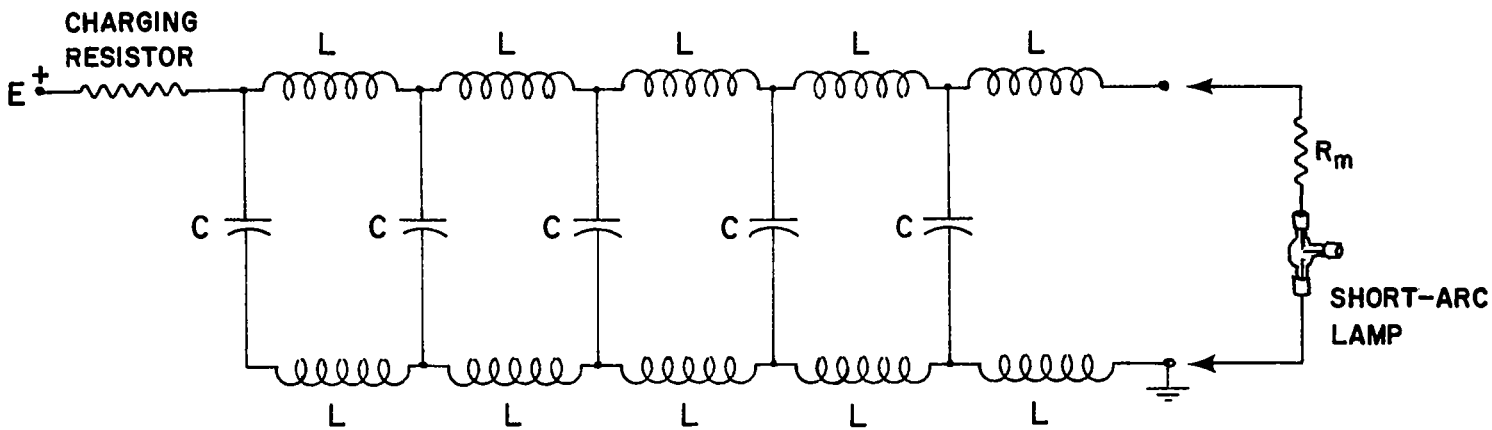

Figure 8.- Typical five-section pulse-forming network.

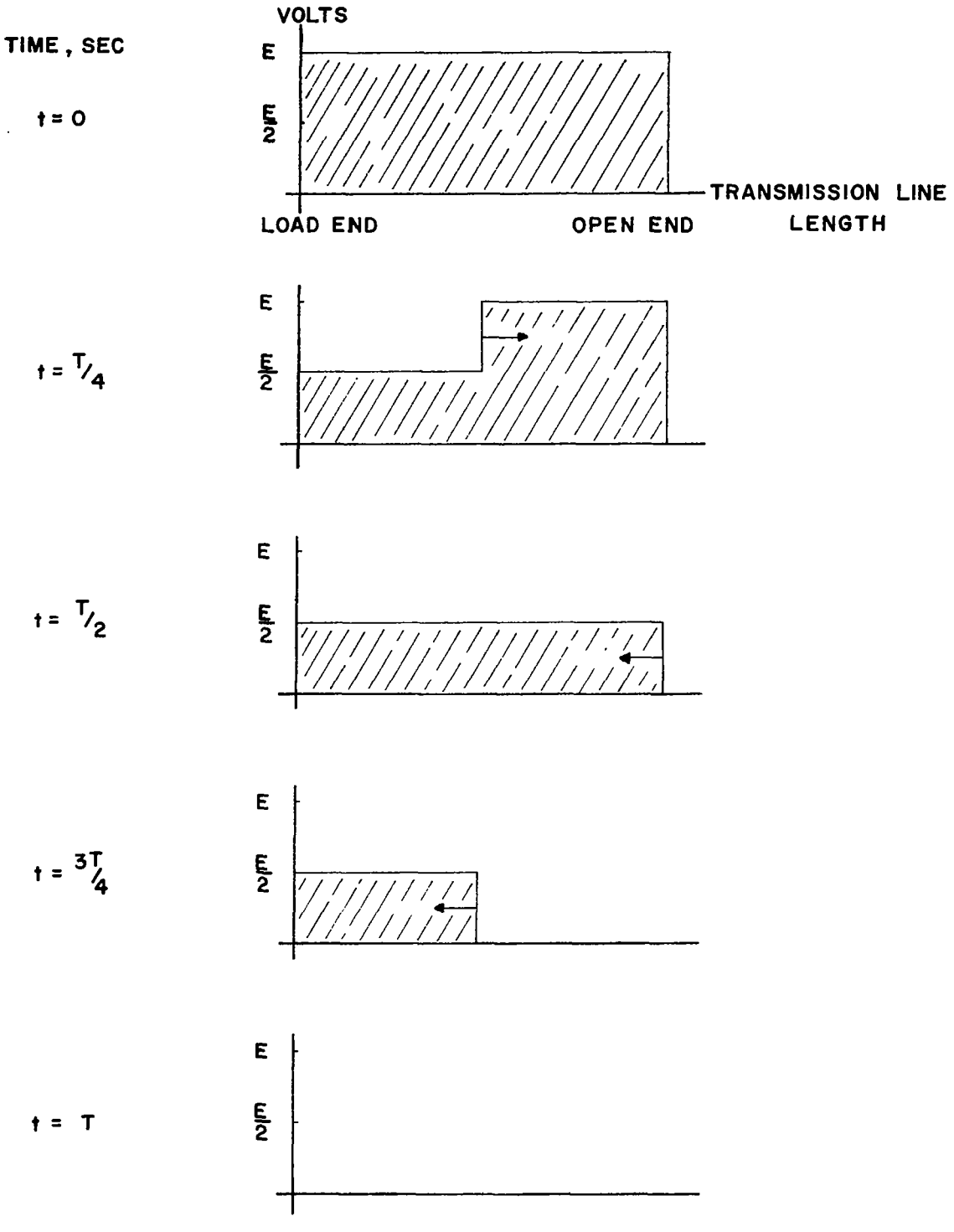

Figure 9.- Discharge mechanism for pulse-forming network with matched load.

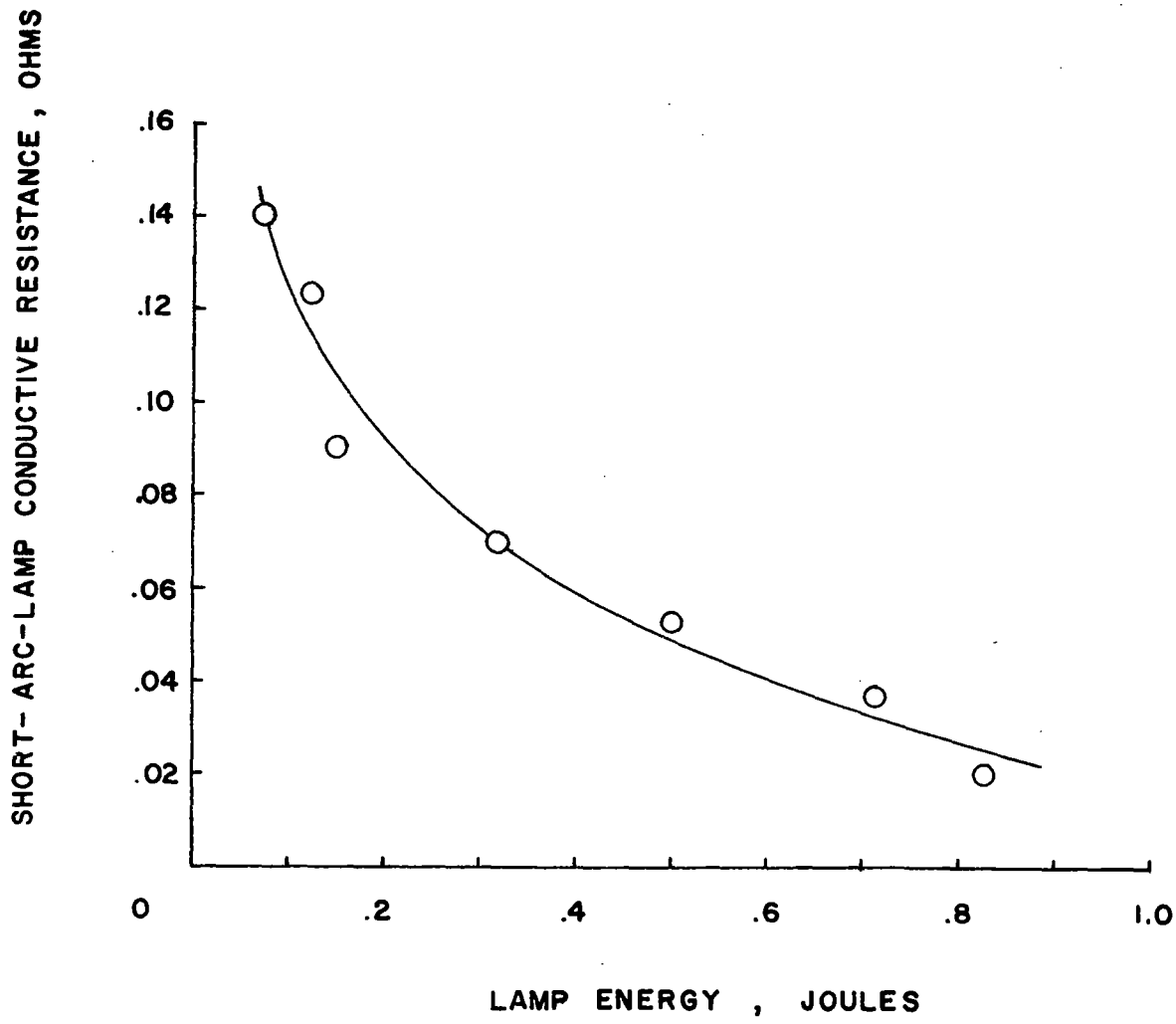

Figure 10.- Variation of resistance with energy for a typical short-arc lamp.

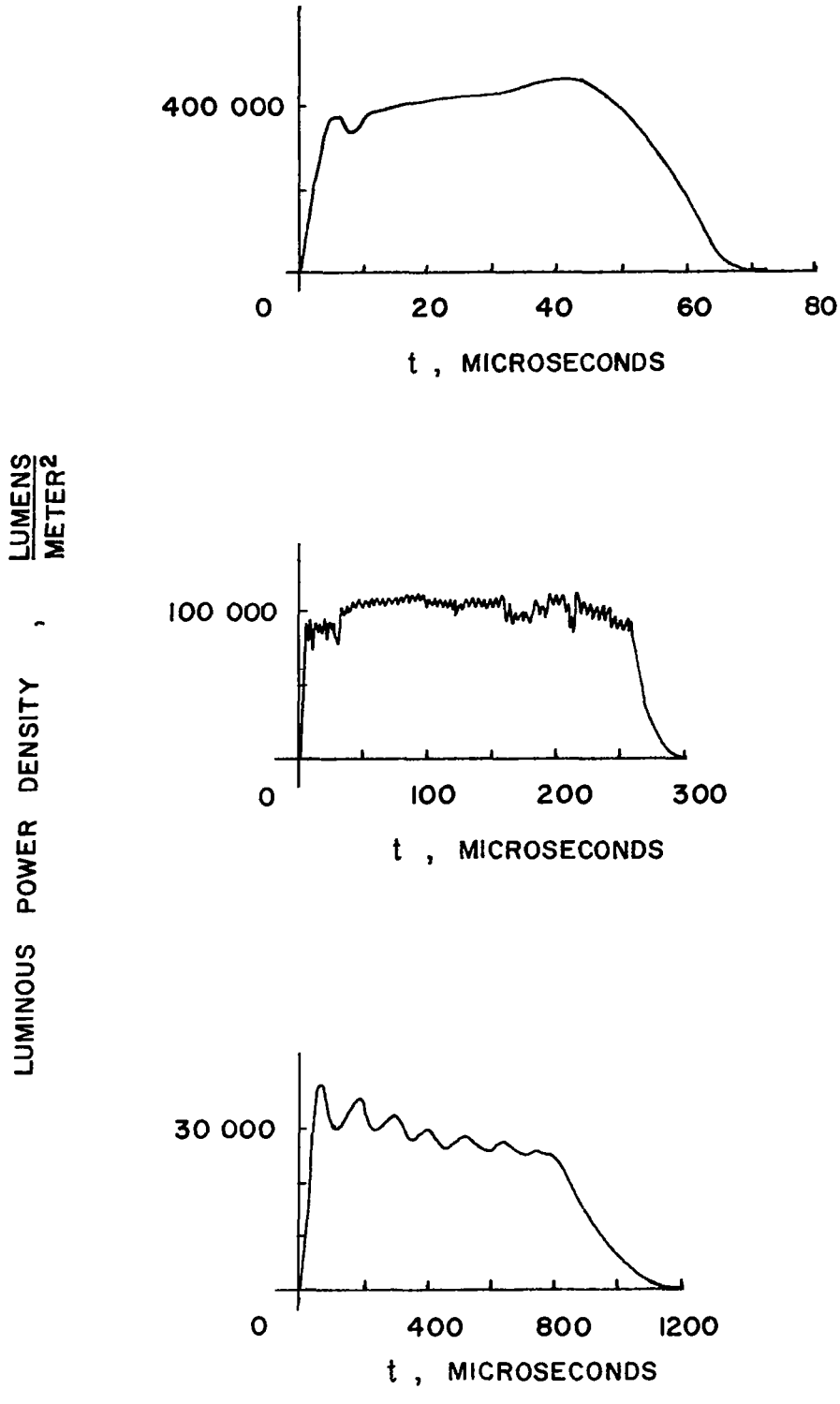

Figure 11.- Typical light pulses of 60 microseconds, 250 microseconds, and 1 millisecond.

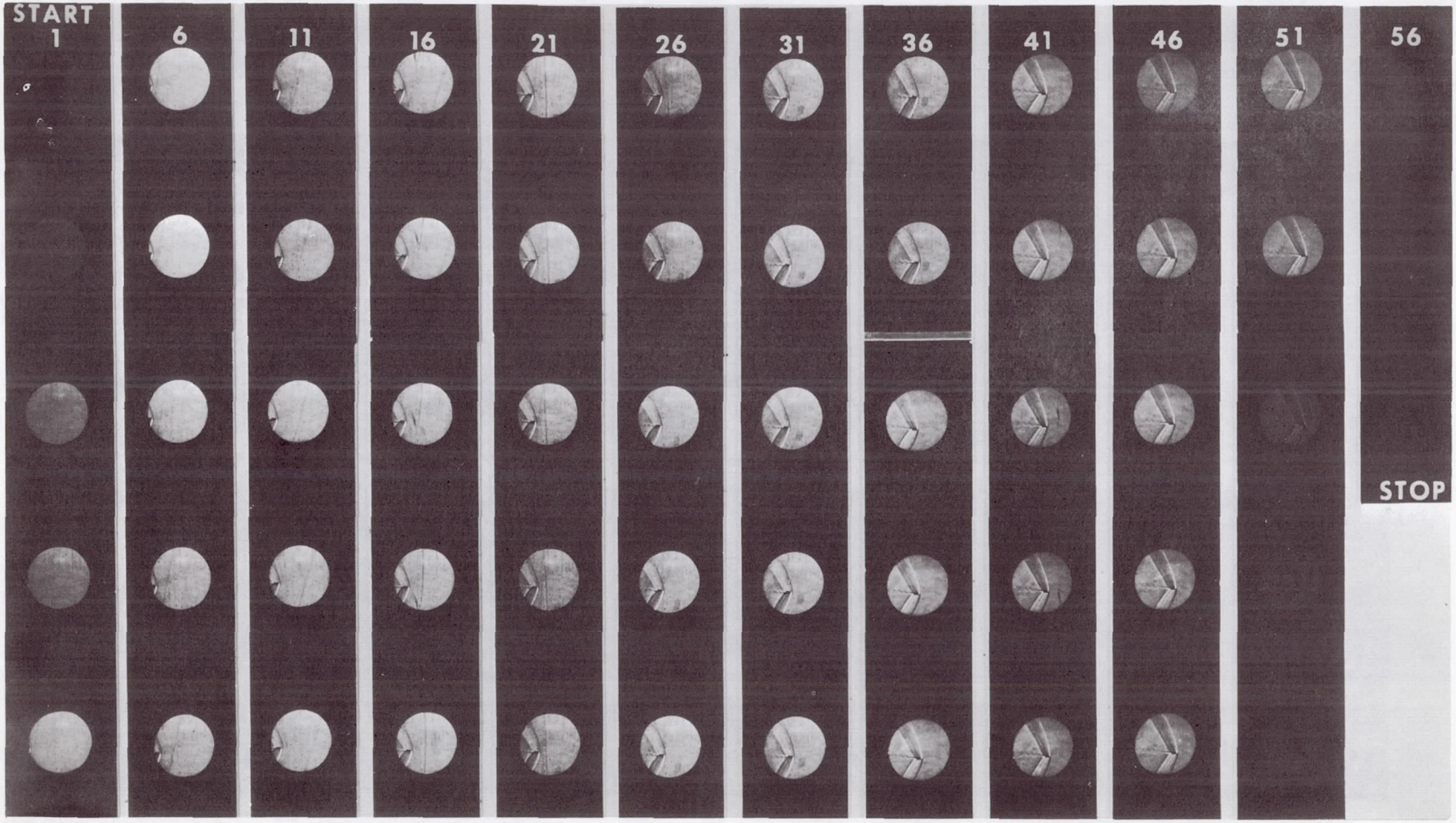

L-68-8514

Figure 12.- Schlieren photographs of a 22-caliber bullet at a velocity of 550 meters/second using the 250-microsecond pulse-forming network.

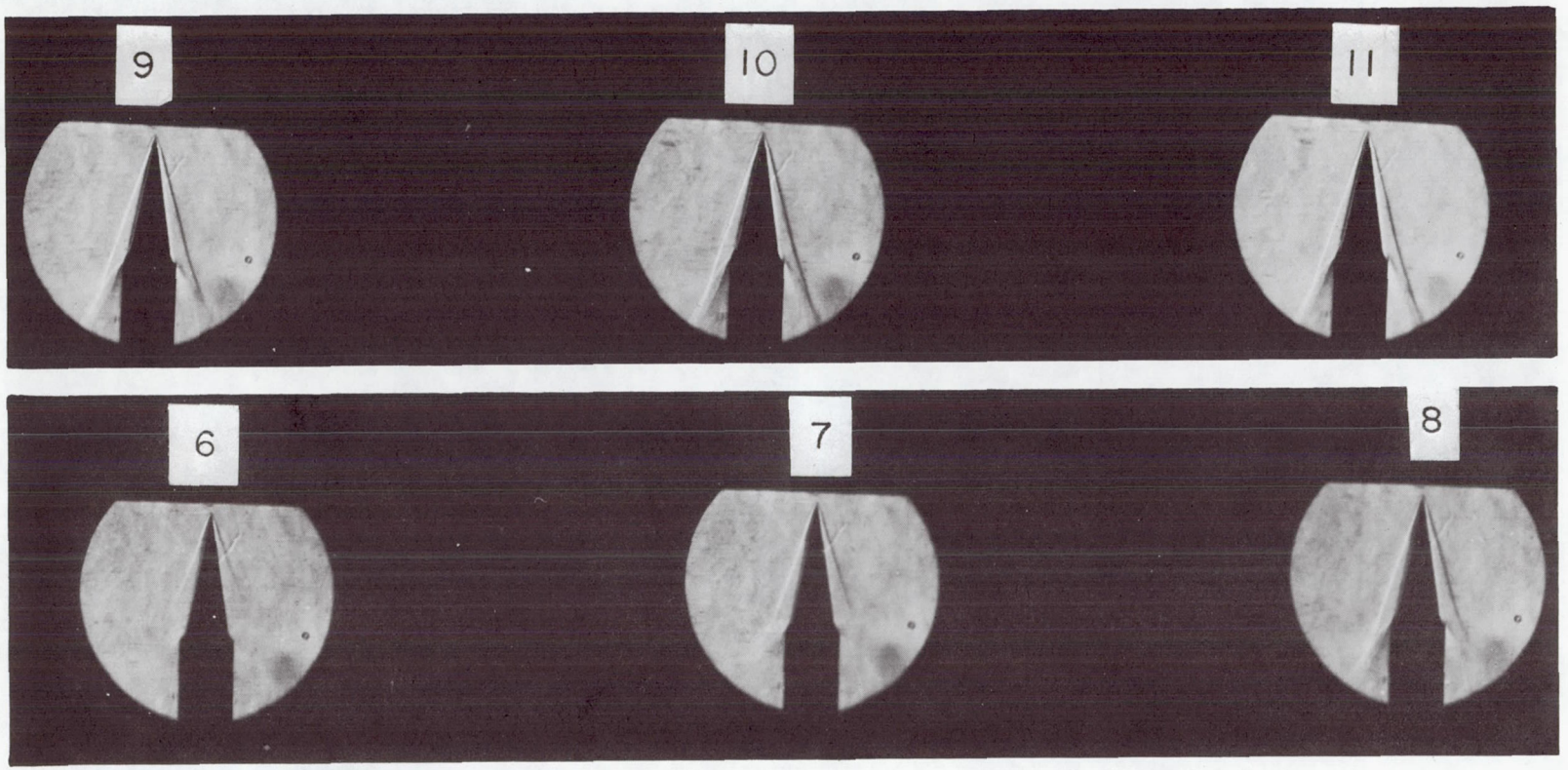

L-68-8515

Figure 13.- Six consecutive schlieren photographs of shock flow at a velocity of 5 kilometers/second around a 10^{o} wedge in the Langley pilot model expansion tube at a density of 0.0176 kilogram/meter^{3} made with 250-microsecond pulse-forming network.

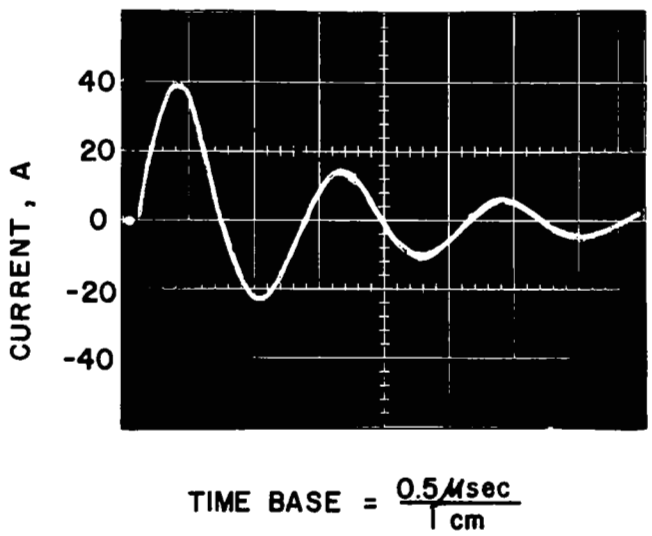

(a) Actual oscilloscope record.

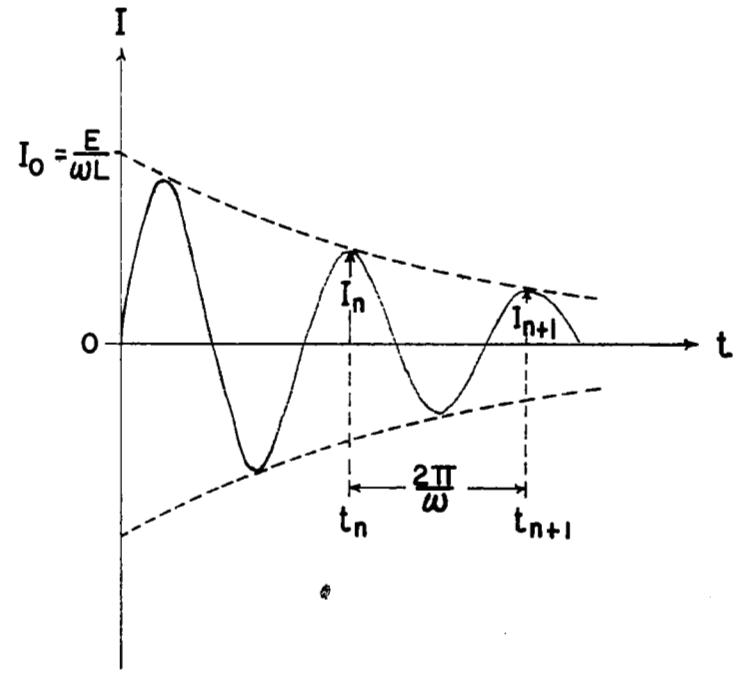

(b) Exponentially damped sinusoidal current.

Figure 14.- Series RLC circuit discharge waveform used to calculate short-arc-lamp conductive resistance.